Power-Law Temperature-Dependence of the London Penetration Depth in YBCO

Tobias Faehndrich
Physics and Astronomy Department, University of British Columbia

(PHYS 409)

(Dated: April 8, 2024)

The exact mechanisms behind high-T_c superconductors are not well understood and thus it is crucial to characterize unconventional superconducting behaviours. The power-law temperature dependance of the London penetration depth is one indicator of topological superconductivity, which could host the theorized Majorana fermion zero modes with important applications in quantum computation. The temperature dependence of London penetration depth, in the high-temperature superconductor $YBa_2Cu_3O_{7-x}$ with x = 0.08 is investigated below a determined critical transition temperature of 92.12 K. A power law relationship $\lambda_L \propto (1 - T/T_c)^n$ where n is fit for the low-temperature regime to $n = -3.74 \pm 0.2$. These results add to the literature on unconventional topological d-wave superconductors.

The discovery of superconductivity [1] in 1911 marked a pivotal moment in physics, revealing a phenomenon where the resistivity of mercury abruptly dropped to zero at a critical temperature (T_c) near 4.2K, coinciding with the transition temperature of liquid helium-4. Since then, a myriad of theoretical models has emerged aiming to better understand the underlying mechanisms governing superconductivity, ranging from the London model [2] and two-fluid model [3] to the celebrated Bardeen-Cooper-Schrieffer (BCS) theory [4]. The BCS theory, predicated on the formation of Cooper pairs arising from electron-phonon interactions, has provided a robust framework for understanding conventional superconductors, predominantly composed of simple atomic compounds.

However, the landscape of superconductivity underwent a paradigm shift with the discovery of high-temperature superconductors (HTSCs) in the 1980s [5], epitomized by the unconventional material $YBa_2Cu3O7 - x$ (YBCO). YBCO defied conventional wisdom by exhibiting superconductivity at temperatures surpassing the boiling point of liquid nitrogen [6]. Despite these advancements, the mechanisms underpinning HTSCs, particularly the formation of Cooper pairs, remain elusive. It is postulated that the superconducting behaviour in HTSCs, facilitated by copper oxide layers within their structures, is intricately linked to doping effects [7, 8].

The Meissner effect, characterized by the expulsion of magnetic flux from the interior of a superconductor upon transitioning to the superconducting state [9], serves as a hallmark property shared by both conventional and unconventional superconductors. The near-perfect diamagnetism exhibited by superconductors underscores their potential for technological applications such as magnetic levitation (maglev) transportation systems [10].

In this study, the fundamental understanding of HTSCs is probed, focusing on shedding light on the mechanisms governing the London penetration depth (λ_L) in YBCO. By exploring the temperature dependence of λ_L and its power-law behaviour, we aim to better understand the complexities of superconductivity in YBCO and contribute to the broader understanding of HTSCs. Consequently, a better understanding of HTSCs will lead to a lowering of costs for major superconductivity applications such as MRIs, cellphone base stations, and quantum computers [11].

The London penetration depth (λ_L) characterizes the exponential decay of the magnetic field and the screening currents within high-temperature superconductors (HTSCs). In general, λ_L can be both temperature and direction dependent.

To measure the Meissner effect, the induced voltage in loops of wires is determined using Faraday's Law, expressed as:

$$V_{\text{loop}} = -\frac{d\Phi}{dt}, \tag{1}$$

where the magnetic flux (Φ) is defined as

$$\Phi = \int \vec{B} \cdot d\vec{a}. \tag{2}$$

An applied AC magnetic field is generated by applying voltage to an outer coil, inducing voltage in two smaller inner coils connected in series but oppositely wound. The sum of induced voltages is minimized to zero in the base case with no Meissner effect, by carefully changing the height of the outer coil, which, if done correctly, centers the sample in one of the inner coils. When YBCO below T_c is introduced into one of the inner coils, some of the AC magnetic field lines are expelled outside of the inner coil, so that the net voltage magnitude increases. Literature [12] provides the relation:

$$|V_{\text{coil}} - V'_{\text{coil}}| = C|\vec{m}| = C' \left(1 - \frac{2\lambda_L}{t}\right), \tag{3}$$

where $|\vec{m}|$ is the magnetization magnitude of the sample, V_{coil} is the voltage in a pickup coil without YBCO sample, V'_{coil} is the other voltage coming from the pickup coil with the YBCO sample inside, C and C' are constants, and t is the thickness of the sample. Using this equation a

normalization of the net voltage is used to get readings of magnetization and subsequently the London penetration depth.

The experimental setup (Figure 1) consisted of a container for the liquid nitrogen, the large outer coil surrounding the container, and a quartz test tube containing the probe. The probe contains the sample along with the 4-wire thermometry circuit and DC heater circuit, along with the two smaller inner coils. The test tube is either filled with Helium gas while heating the sample (for pure gas thermal contact) or pumped out to be an insulating vacuum while cooling the sample down. A digital multimeter (DMM) was used for 4-wire silicon diode thermometry, and connected via a GPIB cable to our PC DAQ LabVIEW program used to collect temperature data. Additionally, a DC power supply is used to supply current to a resistor element placed next to the sample within the apparatus which provides a variable heat source for the sample when taking the temperature dependant measurements. A function generator is used to send an AC signal (10 kHz, 10 V_{pp}) into the outer field coil of the apparatus. It is also referenced into a lock-in amplifier to allow for precise low signal measurements of the resulting μV reading levels. The lock-in amplifier additionally has a GPIB cable connection to send the signals to our PC.

The YBCO test tube was placed into the apparatus and positioned to be centered (with a minimized voltage amplitude reading) inside one of the inner coils. When the YBCO is above T_c, the magnetic field penetrates through the sample without any significant hindrance, and consequently the induced currents in the oppositely wound coils cancel out for a minimized voltage reading. The YBCO is then cooled by adding helium gas to the test tube. This puts the YBCO into thermal contact with the liquid nitrogen (LN) and the sample cools to nearly 77.4 K. Once the temperature of the YBCO drops below it's critical temperature T_c, the Meissner effect expels the magnetic field around the YBCO so that one of the inner coils has less induced currents. This leaves a sudden increase in the net voltage (or the proportional magnetic moment) magnitude reading.

Above T_c, a linear trend is identified in the London penetration depth, coming from a roughly linear reduction in the resistance of the inner coils with temperature. This trend is subtracted from the entire data set since it is a background effect separate from the Meissner Effect of the material. Additionally, a small offset from 0 is found above T_c which likely comes from the inner coils not being perfectly centered in the larger outer coil. Thus the offset is also removed. The data is finally rescaled so that the values go from zero to one, showing $\frac{|\vec{m}(T)|}{|\vec{m}(T_o)|}$ vs T data, since $V \propto |\vec{m}(T)|$ and where $T_o = 80$K. The London penetration depth can be acquired starting from [12],

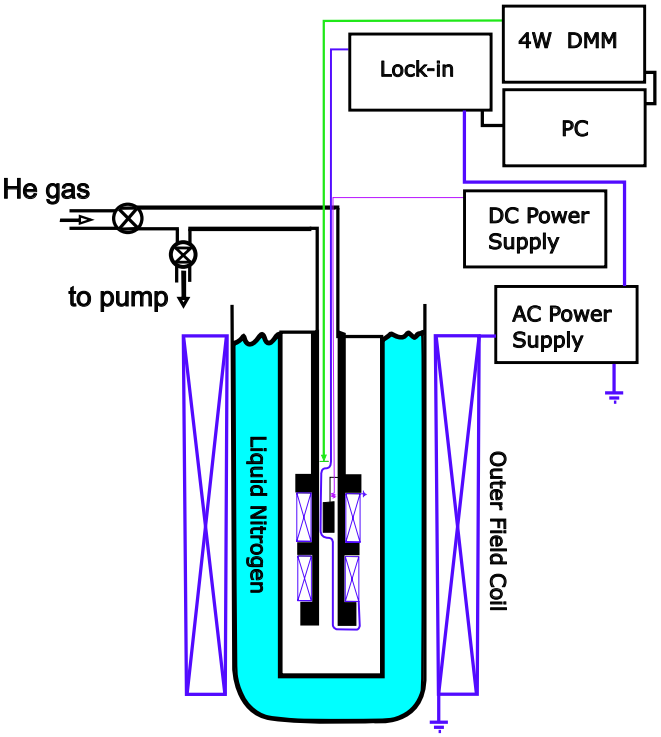

FIG. 1. A circuit schematic of the experimental setup. The AC power supplier gives the outer solenoid voltage and also gives a reference signal to the lock-in amplifier. Two inner oppositely wound wire loops get an induced current and the net absolute voltage gets input into the lock-in amplifier to be filtered. The DMM makes a 4-wire measurement on a diode near the sample to ensure proper temperature measurements. The DC power supply provides a voltage for the resistive heater circuit which can warm up the sample. The DMM and lock-In have GPIB cables that go to the PC for data collection. The figure is inspired from [12].

$$|\vec{m}| \approx l_x l_y t \left(1 - \frac{2\lambda_L}{2}\right) H_{ext}, \tag{4}$$

where l_x, l_y, and t are the sample dimensions and H_{ext} is the external magnetic field and assuming that $\lambda_L \ll t$. Normalizing the magnetization by taking the approximate value of $\lambda_L(80\text{K}) \approx 3000\mathring{A}$, the normalized magnetization expression can be determined

$$\frac{|\vec{m}(T)|}{|\vec{m}(T_o)|} \approx \frac{\left(1 - \frac{2\lambda_L}{2}\right)}{\left(1 - \frac{2(3000\mathring{A})}{2}\right)}. \tag{5}$$

Note that many of the constant parameters from the original expression and cancelled out and λ_L can be simply issolated. The raw data is converted to λ_L and is plotted in Figure 2. At a temperature of $T_c = 92.12$ K the YBCO transitions into a superconducting phase and displays a sharp change in the penetration depth indicating the Meissner effect.

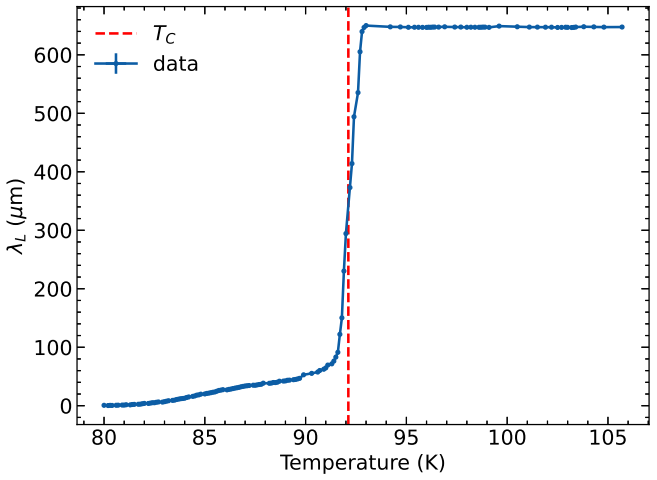

FIG. 2. The London penetration depth (λ_L) is plotted against the temperature with the superconducting transition shown. The London penetration depth is calculated from the voltage signal using the condition of $\lambda_L(80K) \approx 3000\mathring{A}$. Uncertainties are propagated using standard uncertainty rules from the initial measurement uncertainty in the voltage until λ_L.

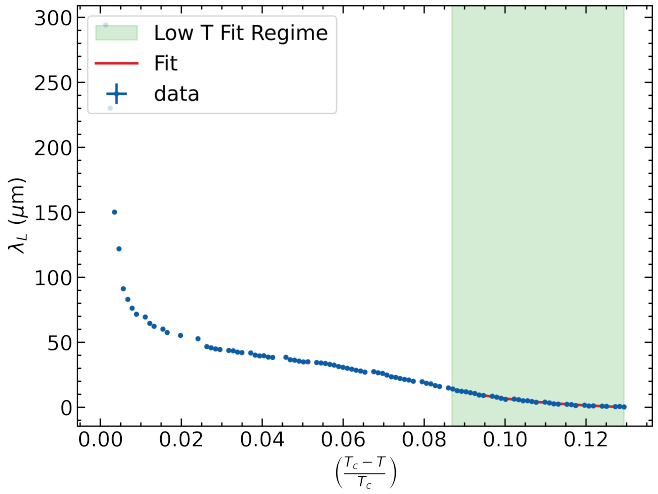

FIG. 3. The temperature is rescaled from Figure 2, with the same London penetration depth (λ_L) y-axis and plotted for the below T_c regime from T_c to T_c-12K where power law behaviour is observed and fitted in the coldest regime shown in as the green dashed line from T_c-12K to T_c-8K. The power law behaviour is $\lambda_L \propto \left(\frac{T_c - T}{T_c}\right)^n$, and fits to a power of $n = -3.74 \pm 0.2$ well.

Beyond T_c there is a distinct regime in the lowest temperature regime where the penetration depth is not constant but rather varies with temperature. The x-axis is rescaled in Figure 3 to have an x-axis of $1 - T/T_c$ and goes from T_c, to T_c-12 K where the coldest regime is fit to a power law,

$$\lambda_L = a\left(\frac{T_c - T}{T_c}\right)^n + b, \tag{6}$$

where n = -3.74 ± 0.2, with uncertainty calculated from the fitting package covariance matrix.

The fitting regime data is then scaled by that power and plotted in Figure 4.

A linear slope is well fit with corresponding residuals, indicating that the data is well-fitted to this power-law relationship. Specifically, the residuals exhibit a random distribution around zero, with no discernible systematic patterns or biases. A required but not sufficient condition for the existence of a gapless Majorana surface fluid can be the signature power-law dependence of $\lambda_L \sim T^3$ [13]. This suggests that since there is enough uncertainty on our measured power law, the YBCO as measured is a possible candidate for new interesting physics that is predicted to be in topological superconductors (TSC) but have eluded scientists to this day. The possible impact lies in the applications of the Majorana zero modes (MZMs) to important applications in quantum computation amongst others [14]. In contrast, other groups have found that strong linear dependence in YBCO at the lowest temperatures (<25K) which was characteristic of the pure d-wave superconductor without any defects [15]. Several other groups find a T^2 dependence with thin films but this may be due to defects in the samples [16–

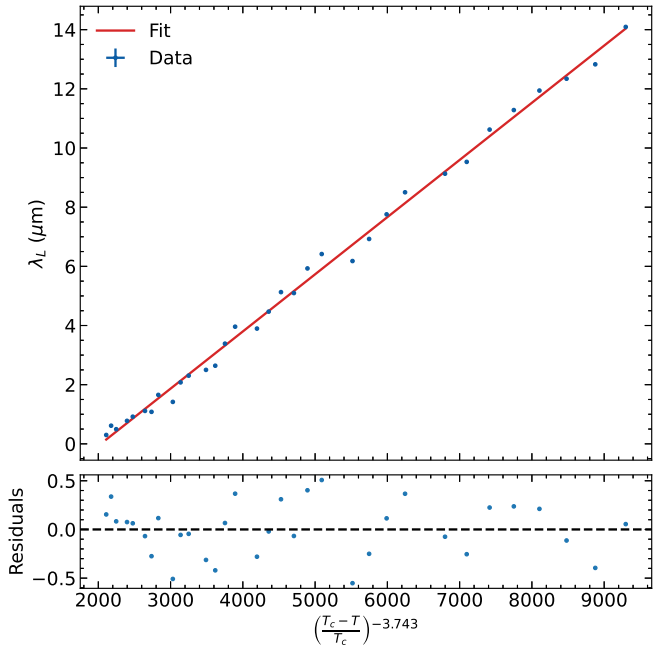

FIG. 4. The plot shows data in the Figure 3 cold fitting range, T_c-12K to T_c-8K, plotted as a function of $(1 - T/T_c)^{-3.743})^3$ and showing the well fitted linear slope showing the correct power law for this data. Additionally the subplot below the data and fit shows the residuals where no discernable trend takes place, which is a sign of a good fit.

19]. It is additionally noted by Hardy et. al. [15] that closer to T_c they find behaviour is unlike either s-wave or d-wave pairing in the weak-coupling limit.

In conclusion, a power law temperature dependence of YBCO in temperatures roughly 12 degrees lower than T_c is observed, which adds useful information to the literature. The behaviour seems to not match well with any previous measurements or exact theories but diverges from the s-wave BCS theory expectation of an exponentially activated temperature dependence. This presents our YBCO sample as truly unconventional. Disagreements are found with the d-wave expectation of a linear dependence likely due to impurities in the YBCO sample, and the fact that the temperature is still relatively high in the experiment. Further work can be done with YBCO in a Helium cryostat down to much lower temperatures to investigate the lower temperature regime. Additionally, further studies may choose to vary the $\lambda_L(80K)$ parameter to see how that changes the characteristics of the relation. Additionally, another parameter that could be investigated in the future is the applied AC voltage amplitude which would correspondingly change the magnetic field amplitude. This study lays important ground-work on the understanding of YBCO and its unconventional nature.

The help of the PHYS 409 teaching team for their insights in the project is acknowledged. Additionally the lab manual was very useful to follow along too. Sergey Frolov's University of Pittsburgh solid state physics lectures and notes as well as the Kittel textbook are acknowledged as they were used for background reading on the topic. LLMs were used very lightly on specific spots in my introduction.

[1] H. Kamerlingh Onnes, Proceedings 13 ii (1911) 1274, Communications of the Physical Laboratory of the University of Leiden (1911).

[2] F. London, H. London, and F. A. Lindemann, The electromagnetic equations of the supraconductor, Proceedings of the Royal Society of London. Series A - Mathematical and Physical Sciences **149**, 71 (1935), https://royalsocietypublishing.org/doi/pdf/10.1098/rspa.1935.0048.

[3] J. Bardeen, Two-fluid model of superconductivity, Phys. Rev. Lett. **1**, 399 (1958).

[4] J. Bardeen, L. N. Cooper, and J. R. Schrieffer, Theory of superconductivity, Phys. Rev. **108**, 1175 (1957).

[5] J. G. Bednorz and K. A. Müller, Possible high T_c superconductivity in the Ba-La-Cu-O system, Zeitschrift fur Physik B Condensed Matter **64**, 189 (1986).

[6] M. K. Wu, J. R. Ashburn, C. J. Torng, P. H. Hor, R. L. Meng, L. Gao, Z. J. Huang, Y. Q. Wang, and C. W. Chu, Superconductivity at 93 k in a new mixed-phase y-ba-cu-o compound system at ambient pressure, Phys. Rev. Lett. **58**, 908 (1987).

[7] X. Ren, J. Li, W. Chen, *et al.*, Possible strain-induced enhancement of the superconducting onset transition temperature in infinite-layer nickelates, Communications Physics **6**, 341 (2023).

[8] X. Luo, H. Chen, Y. Li, *et al.*, Electronic origin of high superconducting critical temperature in trilayer cuprates, Nature Physics **19**, 1841 (2023).

[9] W. Meissner and R. Ochsenfeld, Ein neuer effekt bei eintritt der supraleitfähigkeit, Naturwissenschaften **21**, 787 (1933).

[10] F. Dong, Z. Huang, L. Hao, *et al.*, An on-board 2g hts magnets system with cooling-power-free and persistent-current operation for ultrahigh speed superconducting maglevs, Scientific reports **9**, 11844 (2019).

[11] A. Bussmann-Holder and H. Keller, High-temperature superconductors: underlying physics and applications, Zeitschrift für Naturforschung B **75**, 3 (2020).

[12] UBC, *Lock-in Detection: High-Tc Superconductivity*, University of British Columbia (2024).

[13] T. C. Wu, H. K. Pal, P. Hosur, and M. S. Foster, Power-law temperature dependence of the penetration depth in a topological superconductor due to surface states, Phys. Rev. Lett. **124**, 067001 (2020).

[14] S. D. Sarma, M. Freedman, and C. Nayak, Majorana zero modes and topological quantum computation, npj Quantum Information **1**, 15001 (2015).

[15] W. N. Hardy, D. A. Bonn, D. C. Morgan, R. Liang, and K. Zhang, Precision measurements of the temperature dependence of λ in $yba_2cu_3o_{6.95}$: Strong evidence for nodes in the gap function, Phys. Rev. Lett. **70**, 3999 (1993).

[16] S. M. Anlage and D.-H. Wu, Magnetic penetration depth measurements in cuprate superconductors, Journal of Superconductivity **5**, 395 (1992).

[17] J. Annett, N. Goldenfeld, and S. R. Renn, Interpretation of the temperature dependence of the electromagnetic penetration depth in $yba_2cu_3o_{7-\delta}$, Phys. Rev. B **43**, 2778 (1991).

[18] J. Y. Lee, K. M. Paget, T. R. Lemberger, S. R. Foltyn, and X. Wu, Crossover in temperature dependence of penetration depth λ(t) in superconducting $yba_2cu_3o_{7-\delta}$ films, Phys. Rev. B **50**, 3337 (1994).

[19] D. A. Bonn, R. Liang, T. M. Riseman, D. J. Baar, D. C. Morgan, K. Zhang, P. Dosanjh, T. L. Duty, A. MacFarlane, G. D. Morris, J. H. Brewer, W. N. Hardy, C. Kallin, and A. J. Berlinsky, Microwave determination of the quasiparticle scattering time in $yba_2cu_3o_{6.95}$, Phys. Rev. B **47**, 11314 (1993).